Precipitation Chemistry in Bulgaria During Saharan Dust Outbreaks

Emilia Georgieva, Elena Hristova, and Blagorodka Veleva

Abstract The objective of this work is to investigate the influence of Saharan dust events on the chemical composition of rain samples collected at three sites in Bulgaria during 2017–2018. Saharan dust intrusions were identified through a combination of satellite retrieved aerosol data and results from dust forecasting models and from backward trajectory model. The chemical composition of the samples (acidity pH, conductivity EC, main ions and elements) is analysed in view of the direction of the approaching air masses—"direct" influence (south-west), and "indirect" influence from other directions and regions, already impacted by Saharan dust. The samples were characterised by pH from 4.1 to 7.4, elevated values for EC (max 202 μS cm^{-1}) and for Si, Ca, Fe, Mg concentrations. For cases with direct influence Si and Ca values were up to 1.5 and 25 mg l^{-1}. In most of the indirect cases increased concentrations of sulphate, nitrate and ammonium were observed (up to 39.5, 23.1 and 8.3 mg l^{-1}).

Keywords Precipitation chemistry data · Saharan dust · Satellite AOD

1 Introduction

Sand and Dust Storms are recognized as hazardous meteorological events that impact the society in many ways—soil and agriculture, ecosystems, air quality and human health, aviation, visibility, solar power production and other socio-economical activities. These events present a unique form of natural hazard in that the source and the impact regions can be separated by great distances [1]. Mineral dust particles can be lifted by strong winds from bare dry soils into the atmosphere and being transported

E. Georgieva (✉) · E. Hristova · B. Veleva
National Institute of Meteorology and Hydrology, 66, Tsarigradsko Shose Blvd, 1784 Sofia, Bulgaria
e-mail: emilia.georgieva@meteo.bg

E. Hristova
e-mail: elena.hristova@meteo.bg

B. Veleva
e-mail: blagorodka.veleva@meteo.bg

N. Dobrinkova and G. Gadzhev (eds.), *Environmental Protection and Disaster Risks*, Studies in Systems, Decision and Control 361,
https://doi.org/10.1007/978-3-030-70190-1_18

downwind affecting regions hundreds to thousand kilometers away. It is estimated that between 1000 and 3000 Tg of mineral dust is uplifted into the atmosphere annually, with Saharan desert being the largest global contributor [2]. The atmosphere of the Mediterranean Basin is highly influenced by the Sharan Dust intrusions, as two of the main transport paths of the emitted dust particles is northward to Europe, and eastward to Middle East [3].

The airborne dust particles are removed from the atmosphere by settlement (dry deposition) or are washed out by rains (wet deposition). The last mechanism is prevailing for fine grained particles and distances far-away from the source regions [4]. There are various effects of the deposited dust particles: they are capable of modifying the soil properties, can act as fertilizes in marine ecosystems [5] and can neutralize atmospheric acidity and reduce acid rains, [6]. Although Saharan dust events are detected with higher frequency in the Mediterranean countries and southern Europe, other northern and central parts of the continent are also influenced [7, 8]. The Balkans are not regarded as a dusty region, but the location in the so called D1B zone of the Saharan dust-fall map, [4], implies that Saharan dust can be incorporated in the soil system and change its structure.

The frequency of Saharan Dust outbreaks in Bulgaria is about 20% over annual days, as estimated by 10 years data for particulate matter concentrations with diameter less than 10 μm (PM10) at the regional background station Rozhen in the southern part of the country, [9]. The maximum of Saharan outbreaks towards Bulgaria is in spring and autumn, as found in a recent study based on satellites data for the period 2005–2018, [10]. This study indicates that on average the days with Saharan outbreaks are 10–13 for the months March, April, May, and can be 20 and more for the same months in specific years. As in Bulgaria during spring also the precipitations are frequent, it could be expected that their chemical composition is influenced by Saharan dust. At the National Institute of Meteorology and Hydrology (NIMH) a monitoring network for acidity of precipitations has been established, [11]. In the last years the chemical analysis of the rain water samples was extended with analysis of main ions, macro and microelements, providing, thus, a possibility to investigate the characteristics of precipitation chemistry during Saharan dust outbreaks in the country.

The purpose of this study is to analyse the influence of Saharan dust outbreaks on the chemical composition of rain samples collected at three sites in Bulgaria during field campaigns in 2017–2018. Another objective is to discuss precipitation chemistry in view of typical pathways of the dust loaded air masses.

2 Methodology

The procedures used for the collection of precipitation samples and their chemical analysis, as well as the methods applied for identification of Saharan dust intrusions are briefly outlined.

Fig. 1 Geographical map of Bulgaria with sampling sites (orange square—Sofia, blue triangle—Cherni vruh, red circle—Ahtopol)

2.1 Precipitation Samples and Their Chemical Analysis

The collection of precipitation samples was organised during field campaigns in 2017–2018 at three meteorological stations located in different environment (Fig. 1). Two of the stations are in the western part of the country: urban one—Sofia-NIMH (42.655 N, 23.384 E, 586 m a.s.l.), and a mountain one—peak Cherni Vruh (42.6167 N, 23.2667 E, 2286 m a.s.l.). The third station is rural one in southeast Bulgaria near the Black Sea coast—Ahtopol (42.084 N, 27.952 E, 26 m a.s.l.). Daily precipitation samples in Sofia and Ahtopol were collected with an automatic wet only device (WADOS), at Cherni Vruh a passive bulk sampler was operated, made of polyethylene terephthalate funnel that was washed every day with deionized water to avoid dry deposition.

The collected samples were further analysed for acidity-pH, conductivity-EC, main anions Cl^-, SO_4^{2-}, NO_3^-, cation NH_4^+ and elements Na, K, Mg, Ca, Fe, Si, Zn, Cu. More details and detection limits for the analysed elements are given in [12].

2.2 Identification of Saharan Dust Intrusions

A combination of modelling results and observational data was applied in order to identify the days characterised by Saharan dust outbreaks in Bulgaria in 2017 and 2018. For all the dates with available precipitation chemistry data at the three stations, an analysis was carried out, involving the following information:

- Results for dust optical depth, dust surface concentrations, dust dry and wet depositions forecasted by the models at the Barcelona Supercomputing Centre (BSC)—BSC-DREAM8b [13], NMMB/BSC-Dust [14], the horizontal resolution is 0.3° × 0.3°;
- Results for aerosol optical depth (AOD) and dust surface concentrations, forecasted by the ensemble model at the World Meteorological Organization Sand and Dust Storm Warning Advisory and Assessment System (WMO SDS-WAS) Regional Center for Northern Africa, Middle East and Europe on a grid with resolution 0.5° × 0.5° [15];
- Results for the Dust AOD and total AOD at 550 nm, and PM10 concentrations forecasted by the global CAMS-ECMWF model [16] over Europe on a grid resolution 0.125° × 0.125°, available through the Copernicus Atmosphere Monitoring Service (CAMS) and the European Centre for Medium Weather Forecast (ECMWF) [17];
- Results for dust and PM10 over Europe obtained by the CAMS regional air quality ensemble model, with horizontal resolution 0.1° × 0.1°, [18];
- Maps based on multi-model results at global scale with resolution 0.1° × 0.1° at the Marine Meteorology Division of the Naval Research Laboratory USA (NRL), [19, 20];
- HYSPLIT air mass backward-trajectories [21, 22] calculated at three arrival heights (500, 1500 and 3000 m a.g.l.) for 96 h, using NCEP GDAS meteorological input with resolution 0.5° × 0.5°, and reanalysis data;
- Satellite data for AOD (level 3 MODIS Terra and Aqua globally on a grid 0.1° × 0.1°), for Aerosol absorbing index and Dust optical depth from MetOP satellites;
- Observed PM10 concentrations at two background stations in mountain areas in Bulgaria—Kopitoto (BG0070A, 1321 m a.s.l.) and Rozhen (BG0053R, 1720 m a.s.l.).

3 Results and Discussion

3.1 Selected Dates and Samples

The analysis of the origin of the dust loaded air masses indicated that the daily precipitation samples can be grouped into two main categories—with "direct" influence, i.e. approaching flow from southern directions, mainly from south-west, and with "indirect" influence, associated with other directions and respective regions, already impacted by Saharan dust. Table 1 presents details for the samples used in this study and the type of influence attributed to them.

Table 1 Date, location and type of influence for the precipitation samples used in this study, A—direct influence, B—indirect influence

No	Date	Sofia	ChVruh	Ahtopol	Type
1.	04.06.2017			+	A
2.	06.06.2017		+		A
3.	03.07.2017		+		B
4.	04.07.2017			+	B
5.	20.09.2017		+		A
6.	07.02.2018	+			A
7.	08.02.2018			+	A
8.	02.03.2018	+			A
9.	05.03.2018			+	A
10.	06.03.2018	+			A
11.	19.03.2018		+		A
12.	20.03.2018		+		A
13.	20.03.2018			+	A
14.	21.03.2018	+			A
15.	22.03.2018	+			A
16.	23.03.2018	+			B
17.	23.03.2018			+	B
18.	28.03.2018			+	A
19.	06.04.2018	+			A
20.	16.04.2018	+			A
21.	24.04.2018	+			B
22.	24.04.2018		+		B
23.	05.05.2018	+			B
24.	10.06.2018	+			B
25.	15.06.2018			+	B
26.	30.06. 2018		+		B

3.2 Examples for Type A and Type B of Saharan Dust Outbreaks

We show here results as maps and precipitation chemistry data for two typical cases/days influenced by Saharan outbreaks of type A and type B.

The first case (16.04.2018) was characterized by dust loaded air masses approaching Bulgaria from south-west (A). The forecast by the SDS-WAS ensemble model (Fig. 2a) showed that the Dust AOD extends over the whole Balkan Peninsula. The accumulated dust wet depositions, estimated by the NMMB/BSC-Dust model

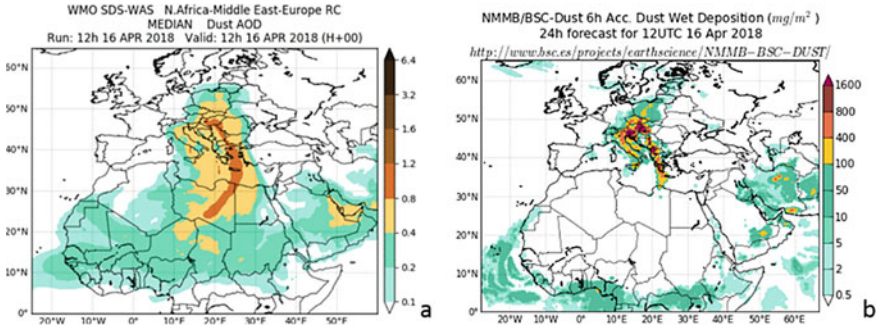

Fig. 2 Case 16.04.2018: **a** median dust AOD from SDS-WAS ensemble model; **b** dust wet deposition from NMMB/BSC-dust model

(Fig. 2b) was concentrated in the western part of the Balkan Peninsula, indicting, thus, that the sampling sites Sofia and Cherni Vruh might be influenced.

The origin of the air masses arriving in Sofia at altitudes 1500 and 3000 m a.g.l, was in Northern Africa, as suggested by the HYSPLIT back-trajectories (Fig. 3a). The Dust AOD, retrieved by the IASI instrument on MetOpA satellite, shows higher values south of Bulgaria and in the eastern parts of the country (Fig. 3b). Satellite data were missing over most of the Balkans (white areas) due to the presence of clouds and rain.

The chemical composition of the precipitation sample from Sofia is shown in Fig. 4. For this case the total ionic concentration (TIC) in the precipitation sample was 54.1 mg.l^{-1}, and consisted from 79% of the following elements: nssSO_4^{2-}, NO_3^- and Ca. The pH and EC values of this sample were very high (7.4 and 132.7 μS cm^{-1}). The most abundant element was Ca followed by nssSO_4^{2-} and NO_3^-.

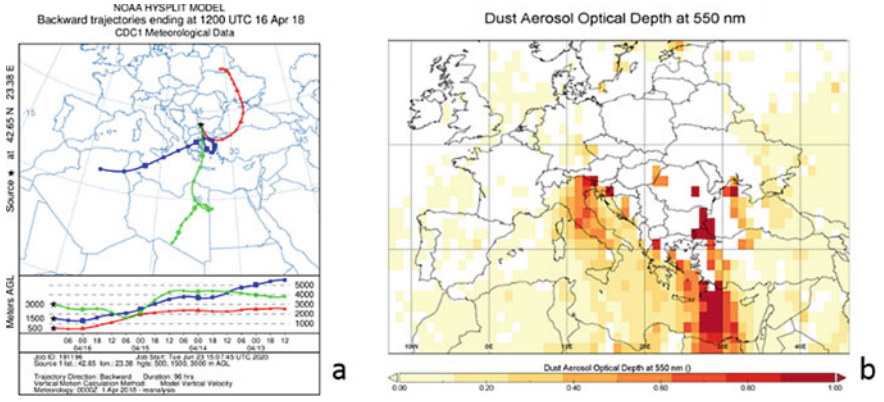

Fig. 3 Case 16.04.2018: **a** HYSPLIT back trajectories, and **b** dust AOD a from IASI instrument on MetOpA

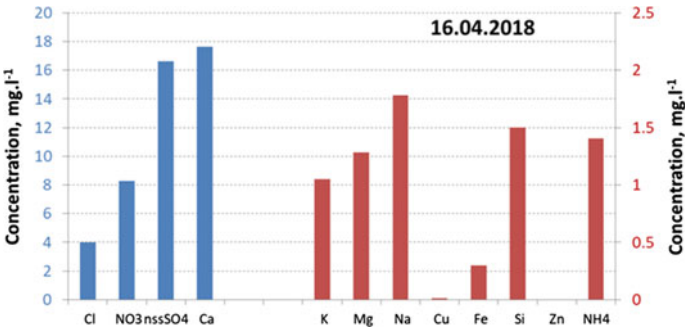

Fig. 4 Concentrations of elements in precipitation sample from Sofia on 16 April 2018

The concentrations of Si, K and Mg were also high, with contribution to the TIC of 3%, 2% and 2%, respectively. The contribution of NH_4^+ is 3%.

The second case (30.06.2018) was characterised by an intrusion from north, north-west towards Bulgaria, but the regions in Central and Western Europe were impacted by Saharan dust few days before. Thus, indirect influence of dust loaded air masses was expected (B). The models at BSC and the system CAMS-ECMWF suggested transport of dust loaded air masses from Northern Africa towards western and central Europe (Fig. 5a, b). Satellite data were limited in Eastern Europe due to cloudiness (Fig. 6b), however the dust transport towards the western part of the continent was well evident. The HYSPLIT back trajectories for the sampling site Cherni Vruh, presented as frequencies for the period 22.06–30.06.2018 in Fig. 6a, indicate that the air masses were from north and north-westerly directions, but also from southern direction.

The chemical composition of the precipitation sample from Cherni Vruh for this second case (Fig. 7) is characterised by high concentrations of $nssSO_4^{2-}$, Ca, K and NH_4^+. The measured pH and EC are 4.9 and 50 μS cm^{-1}. The TIC is 48.5 mg l^{-1}

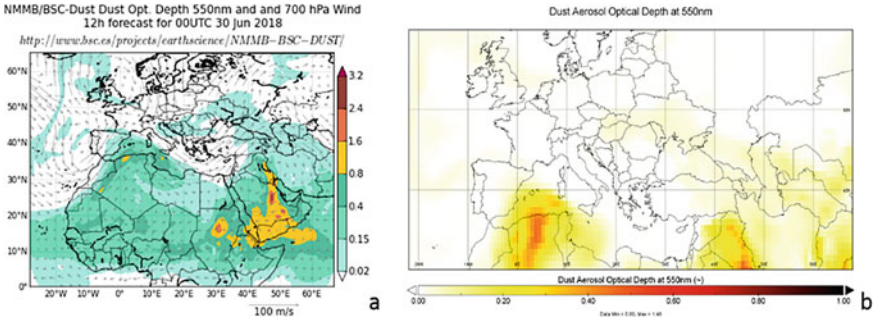

Fig. 5 Case 30.06.2018 (type B): **a** dust AOD and wind vectors at 700 hPa from NMMB/BSC-dust model; **b** dust AOD from CAMS-ECMWF model on 29.06.18 at 18:00 UTC

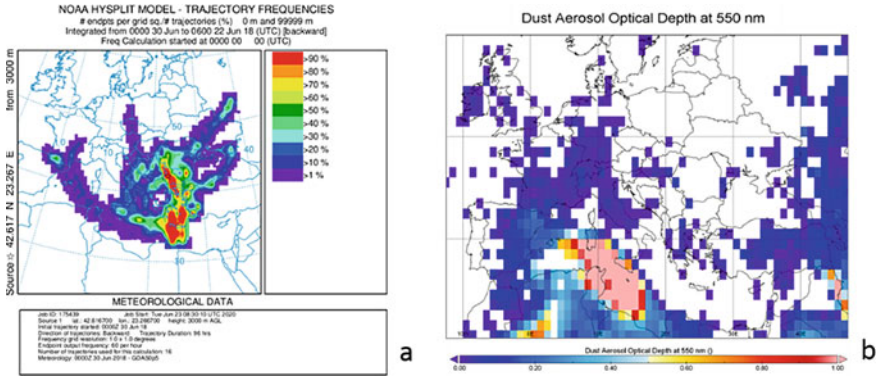

Fig. 6 Case 30.06.2018 (type B): **a** HYSPLIT frequency of back trajectories (22.06–30.06.18), and **b** dust AOD from IASI instrument on MetOpA

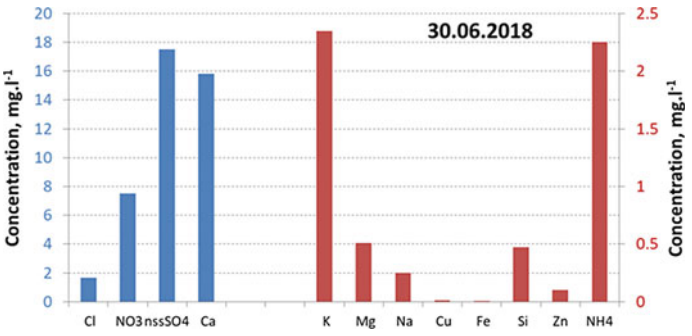

Fig. 7 Concentrations of elements in precipitation sample from Cherni Vrah on 30 June 2018

composed from 84% of the following elements: $nssSO_4^{2-}$, NO_3^- and Ca. The contribution of NH_4^+ is 5% and of Si is only 1%.

Comparing the chemical analysis data for these two samples belonging to the groups A and B, one can notice that for the first one (A-type, or direct influence) the values of Cl^-, Mg, Na and Si were higher, for the second case (B-type, indirect influence) NH_4^+ values were higher. Common for both samples are the high values of $nssSO_4^{2-}$ and Ca.

Before discussing the average precipitation chemistry data for the two groups A and B, synoptic parameters and aerosol loads for the two groups were investigated through composite maps, i.e. maps representing all days in the group.

3.3 Composite Maps for the Groups A and B

The synoptic situation for the two groups was analysed using the National Centers for Environmental Prediction/National Center for Atmospheric Research (NCEP/NCAR) Reanalysis—2 global dataset, [23].

Composite daily maps for Europe were constructed to highlight the main features typical for the two groups. The geopotential height at 700 hPa, the wind vectors and speed at 700 hPa, and the columnar precipitable water amount are shown in Fig. 8. The level 700 hPa (around 3000 m a.s.l.) was selected as the dust transport occurs mainly aloft, [24].

The geopotential height at 700 hPa for group A indicated low pressure system over Central Europe and a center with higher pressure over the southern Mediterranean and North Africa, that led to south-westerly flows towards Bulgaria (Fig. 8a, c). For the group B a high pressure ridge extended from North Africa towards the western and central part of Europe, while there was a low pressure trough over south-eastern Europe that led to flow from northern origin towards Bulgaria (Fig. 8b, d). The winds at 700 hPa over the Balkans were stronger for the A group. The columnar precipitable water amount for group A had higher values in a region south of Bulgaria, while for group B the precipitation region was more wide spread, extending to the west, north and east of the country.

The horizontal distribution of the dust aerosols for the two groups was analysed using the CAMS-ECMWF global model [15, 16] forecasted values for the respective days. The maps for the average Dust AOD for the two groups (Fig. 9 a, b) showed the dust load south of the country for A, and enhanced dust load north-west of the country for B. The maps for the sulphate AOD (Fig. 9 c, d) indicated higher load over Bulgaria and south of the country for group A, while for the group B the sulphate rich areas were extended to the north-west and north of the country.

3.4 Precipitation Chemistry Analysis

The pH frequency distribution (Fig. 10) shows that about 70% of all samples (both groups) were in the neutral and acidity range.

The pH values ranged from 4.1 to 7.4.40% of the precipitation samples in A were in the acidity range (pH < 5.0), 6.7%—in the slightly acidic range (5.0–5.5) and 6.7%—in the alkaline range (>7.0). The pH frequency analysis for B samples showed that in 30% pH was in the range 4.5–5.0, 10% were in the slightly acidic range, and 20% were in slightly alkaline range. pH value higher than 6.2 were not observed for B samples. pH values in the neutral range are observed in 40% for B samples, and in 33% for A samples.

The mean pH value for both groups of samples from Sofia is 6.05 and is higher than the average multiyear pH (5.12) estimated from the precipitation chemistry network

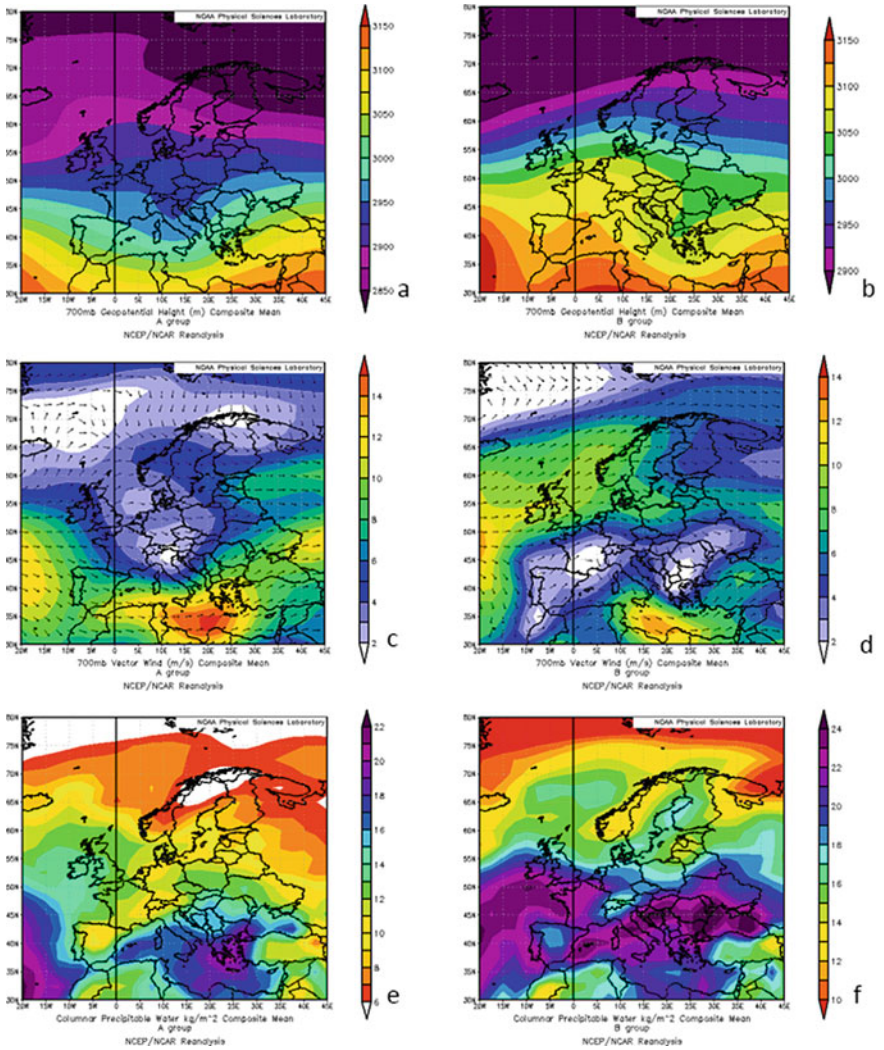

Fig. 8 Synoptic situation–composite maps for group A (left) and group B (right): **a**, **b** geopotential height (m) at 700 hPa; **c**, **d** wind vectors (arrows) and wind speed, (ms^{-1}) at 700 hPa; and **e**, **f** columnar precipitable water (kgm^{-2})

for the period 2002–2019. The same is observed for the samples from Ahtopol—mean for both groups pH is 5.34, while the multiyear one is 5.16.

Some statistical parameters (mean, standard deviation, minimum and maximum) were estimated for the pH and EC, the precipitation chemistry elements and the TIC, for the samples defined as A and B (Table 2).

The contribution of different elements in both A and B samples to the total ionic concentration is presented in Fig. 11. The most abundant ionic species for samples

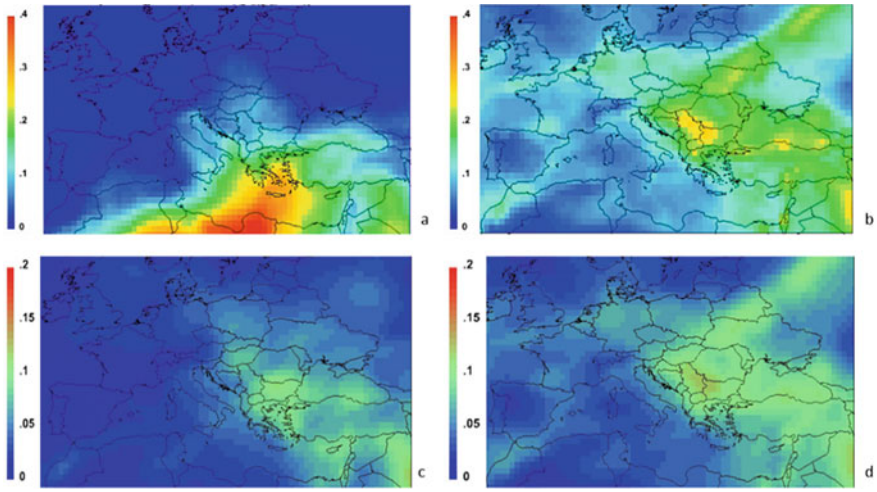

Fig. 9 CAMS-ECMWF averaged maps for A (left) and B (right): **a**, **b** dust AOD, **c**, **d** sulphate AOD, (Generated using Copernicus Atmosphere Monitoring Service Information (2020)

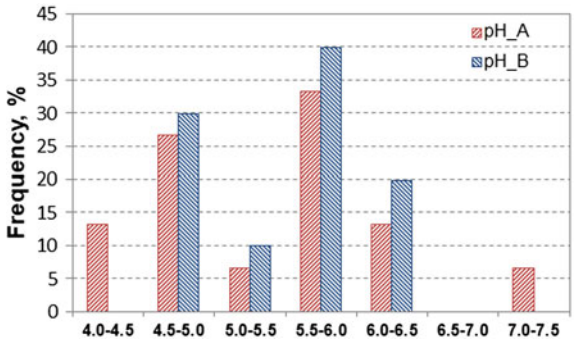

Fig. 10 Frequency distribution of pH for samples in A (red) and B (blue)

in both categories was $nssSO_4^{2-}$, followed by Cl^- and Ca for A category, and Ca and NO_3^- for B category.

The total ionic concentration in both A and B samples consisted mainly of $nssSO_4^{2-}$, NO_3^- and NH_4^+ (A—44% and B—58%). For the group A (flow mainly from south-west) the air masses passing over the Mediterranean Sea were enriched with sea salt aerosol. The evident high correlation between the elements Cl and Na (0.99) conferred this. 31% of the TIC consisted of Cl and Na. The percentage of terrigenous elements (Ca, K, Mg and Si) of the TIC in the A samples is 23.3%. High correlation was obtained also between Ca and Si (0.90), Ca and Fe (0.84), and between $nssSO_4^{2-}$ and Ca (0.73).

The higher contribution of sulphates, nitrates and ammonium ions in B samples can be explained by the enrichment of air masses with substances of anthropogenic origin. The correlations between $nssSO_4^{2-}$ and NH_4^+ (0.7), and between NO_3^- and

Table 2 Statistics (mean, standard deviation, minimum and maximum) for the samples in A ($N = 16$) and B ($N = 10$), concentrations in mg.l^{-1}

Element mg.l^{-1}	Mean A	SD A	Min A	Max A	Mean B	SD B	Min B	Max B
pH (−)	5.5	0.9	4.1	7.4	5.5	0.5	4.7	6.2
EC (μS/cm)	38.7	34.1	16.4	132.7	29.8	22.5	7.4	76.0
Cl	4.55	7.04	0.44	26.94	1.67	1.93	0.11	6.41
NO_3	3.09	3.96	0.17	15.83	4.52	4.84	0.88	15.75
SO_4	5.91	5.54	1.67	20.28	5.93	5.45	0.41	17.55
$nssSO_4$	5.64	5.40	1.59	19.70	5.88	5.44	0.41	17.52
Ca	3.89	4.66	1.07	17.66	4.59	5.03	0.75	15.83
K	1.20	2.37	0.08	8.87	0.79	0.74	0.23	2.35
Mg	0.46	0.42	0.14	1.40	0.34	0.24	0.06	0.86
Na	2.40	4.27	0.11	15.64	0.48	0.86	0.10	2.60
Cu	0.02	0.02	0.01	0.05	0.01	0.00	0.01	0.01
Fe	0.06	0.09	0.01	0.30	0.02	0.02	0.00	0.05
Si	0.28	0.36	0.06	1.50	0.24	0.16	0.07	0.55
Zn	0.11	0.24	0.01	0.81	0.05	0.04	0.01	0.11
NH_4	0.90	1.00	0.13	3.90	0.92	0.80	0.06	2.33
TIC	22.28	22.28	6.58	68.87	18.72	16.95	2.53	48.50

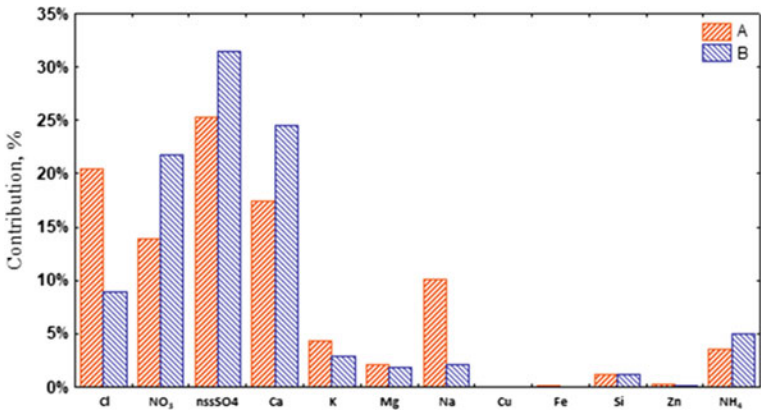

Fig. 11 Contribution (in %) of different elements in precipitation samples for A and B groups

NH_4^+ (0.9) indicate contribution from secondary formed aerosols ($(NH_4)_2SO_4$ and NH_4NO_3).Very high correlations were found between $nssSO_4^{2-}$ and Ca (0.91), and between Ca and K (0.95), indicating that the main source of those ions are from terrigenous origin (e.g. gypsum—$CaSO_4$), [25]. 30.4% of the TIC for the samples of B group consisted of Ca, K, Mg, and Si.

The t-test performed for the mean elemental contributions in the two groups returned a value of 0.035 for the two-tailed *p*-value, indicating, thus, to statistically significant differences between the two groups. Having in mind that the samples are low in number, we recognize that more robust statistical results could be obtained after collecting and analyzing more precipitations samples in different synoptic situations.

The chemical analysis of all samples confirmed that the precipitation associated with dust intrusions is characterized by higher concentrations of terrigenous elements. In both types of intrusions the correlation between $nssSO_4^{2-}$ and Ca was relatively high, indicating similar source of origin.

4 Conclusions

We have analysed the influence of Saharan dust events on the chemical composition of 26 rain samples collected at three sites in Bulgaria during 2017–2018. The samples were divided into two categories with respect to the path of the approaching dust loaded masses: group A (flow from south, south-west; direct influence) and B (flow from north, north-west; indirect influence). The analysis of composite maps for synoptic variables and aerosol optical depth highlighted the regions with dust loaded air masses approaching the country for the days of the two groups. The mean pH of the samples from both groups was 5.5. About 70% of all samples were in the neutral and acidity range. For the sampling site Sofia the mean pH of all samples (6.05) was higher than the multi-year one (5.12) indicating that, in general Saharan intrusions contribute to more alkaline character of precipitations, although for single events this value might be in the acidity range. The precipitation associated with dust intrusions from both groups is characterized by higher concentrations of terrigenous elements (Ca, Si, K). The concentrations of chloride, magnesium and sodium were significantly higher for A samples, as a consequence of the influence of the Mediterranean Sea on the air masses in this group. For the B samples higher concentrations of sulphates, nitrates and ammonium ions was found, suggesting enrichment of air masses with anthropogenic pollutants. The preliminary results, presented here, showed that the trajectory of the air masses is an important factor for the chemical composition of precipitations in Bulgaria. Additional data from sampling are needed, however, in order to extend the analysis and to perform more robust statistical estimates.

Acknowledgements This study was inspired by COST CA16202 “inDust”, and was funded by the Bulgarian National Science Fund through contract N. DN-04/4-15.12.2016. The Copernicus Atmosphere Monitoring Service is acknowledged for providing analysed and forecasted model data on atmospheric chemistry. We are thankful also to model groups for providing operational dust products and maintaining archives—Barcelona Supercomputing Center, WMO SDS-WAS NAMEE Centre and the Marine Meteorology Division of U.S. Naval Research Laboratory, as well as NOAA-ARL for the HYSPLIT on-line platform. We acknowledge also the provider of satellite data observations (ESA, EUMETSAT, NASA/LANCE).

References

1. Middleton, N., Tozer, P., Tozer, B.: Sand and dust storms: underrated natural hazards. Disasters **43**, 390–409 (2019)
2. Prospero, J.M., Ginoux, P.M., Torres, O., Nicholson, S.E., Gill, T.E.: Environmental characterization of global sources of atmospheric soil dust identified with the Nimbus-7 Total Ozone Mapping Spectrometer (TOMS) absorbing aerosol product. Rev. Geophys. **40**(1), 1002 (2002)
3. Goudie, A.S., Middleton, N.J.: Desert Dust in the Global System. Springer, Berlin, Heidelberg (2006)
4. Stuut, J.-B.W., Smalley, I., O'Hara-Dhand, K.: Aeolian dust in Europe: African sources and European deposits. Quat. Int. **198**, 234–245 (2009)
5. Maher, B.A., Prospero, J.M., Mackie, D., Gaiero, D., Hesse, P.P., Balkanski, Y.: Global connections between Aeolian dust, climate and ocean biogeochemistry at the present day and at the last glacial maximum. Earth Sci. Rev. **99**, 61–97 (2010)
6. Rogora, M., Mosello, R., Marchetto, A.: Long-term trends in the chemistry of atmospheric deposition in northwestern Italy: the role of increasing Saharan dust deposition. Tellus B **56**, 426–434 (2004)
7. Klein, H., Nickovic, S., Haunold, W., Bundke, U., Nillius, B., Ebert, M., Weinbruch, S., Schuetz, L., Levin, Z., Barrie, L.A., Bingemer, H.: Saharan dust and ice nuclei over Central Europe. Atmos. Chem. Phys. **10**, 10211–10221 (2010)
8. Varga, Gy., Kovács, J., Újvári, G.: Analysis of Saharan dust intrusions into the Carpathian Basin (Central Europe) over the period of 1979–2011. Global Planet **100**, 333–342 (2013)
9. Pey, J., Querol, X., Alastuey, A., Forastiere, F., Stafoggia, M.: African dust outbreaks over the Mediterranean Basin during 2001–2011: PM10 concentrations, phenomenology and trends, and its relation with synoptic and mesoscale meteorology. Atmos. Chem. Phys. 1395–1410 (2013)
10. Dimitrova, M., Trenchev, Pl., Georgieva, E., Neykova, N., Neykova, R., Nedkov, R., Gochev, D., Syrakov, D., Veleva, B., Atanassov, D., Spassova, T.: Seasonal changes of aerosol pollutants over Bulgaria. In: Proceedings of the 15th International Science Conference Space, Ecology, Safety, SES 2019, SRTI-BAS, Sofia, pp. 241–252 (2019). ISSN 2603-3321
11. Hristova, E.: Chemical composition of precipitation in urban area. Bulgarian J. Meteorol. Hydrol. **22**(1–2), 41–49 (2017)
12. Hristova, E., Veleva, B., Georgieva, E., Velchev, K.: Cloud and rain water chemical composition at peak Cherni Vrah, Bulgaria (in this Book) (2020)
13. Basart, S., Pérez, C., Nickovic, S., Cuevas, E., Baldasano, J.M.: Development and evaluation of the BSC-DREAM8b dust regional model over Northern Africa, the Mediterranean and the Middle East. Tellus B **64**, 1–23 (2012)
14. Pérez, C., Haustein, K., Janjic, Z., Jorba, O., Huneeus, N., Baldasano, J.M., Black, T., Basart, S., Nickovic, S., Miller, R.L., Perlwitz, J., Schulz, M., Thomson, M.: An online mineral dust aerosol model for meso to global scales: model description, annual simulations and evaluation. Atmos. Chem. Phys. **11**, 13001–13027 (2011)
15. WMO SDS-WAS Homepage. https://sds-was.aemet.es/. Last accessed 2020/09/10
16. Benedetti, A., Morcrette, J.-J., Boucher, O., Dethof, A., Engelen, R.J., Fisher, M., Flentjes, H., Huneeus, N., Jones, L., Kaiser, J.W., Kinne, S., Mangold, A., Razinger, M., Simmons, A.J., Suttie M., GEMS-AER team: Aerosol analysis and forecast in the ECMWF integrated forecast system. Part II: data assimilation. J. Geophys. Res. **114**, D13205 (2009)
17. CAMS-ECMWF Homepage. https://apps.ecmwf.int/datasets/data/cams-nrealtime/levtype=sfc/. Last accessed 2020/09/10
18. Marécal, V., Peuch, V.-H., Andersson, C., Andersson, V, Arteta, J., Beekmann, M., Benedictow, A., Bergström, V, Bessagnet, B., Cansado, A., Chéroux, V, Colette, A., Coman, A., Curier, R.L., Denier van der Gon, H.A.C., Drouin, A., Elbern, H., Emili, E., Engelen, R.J., Eskes, H.J., Foret, G., Friese, E., Gauss, M. et al.: A regional air quality forecasting system over Europe: the MACC-II daily ensemble production. Geosci. Model Dev. **8**, 2777–2813 (2015)

19. Xian, P., Reid, J.S., Hyer, E.J., et al.: Current state of the global operational aerosol multi-model ensemble: an update from the international cooperative for aerosol prediction (ICAP). Q. J. R. Meteorol. Soc. **145**, 176–209 (2019)
20. NRL/Monterey Aerosol Page. https://www.nrlmry.navy.mil/aerosol/. Last accesses 2020/09/10
21. Stein, A.F., Draxler, R.R., Rolph, G.D., Stunder, B.J.B., Cohen, M.D., Ngan, F.: NOAA's HYSPLIT atmospheric transport and dispersion modeling system. Bull. Amer. Meteor. Soc. **96**, 2059–2077 (2015)
22. Rolph, G., Stein, A., Stunder, B.: Real-time Environmental applications and display system: READY. Environ. Model Softw. **95**, 210–228 (2017)
23. Kalnay, E., Kanamitsu, M., Kistler, R., Collins, W., Deaven, D., Gandin, L., Iredell, M., Saha, S., White, G., Woollen, J., et al.: The NCEP/NCAR 40-year reanalysis project. Bull. Am. Meteorol. Soc. **77**, 437–472 (1996)
24. Nabat, P., Somot, S., Mallet, M., Sevault, F., Chiacchio, M., Wild, M.: Direct and semi-direct aerosol radiative effect on the Mediterranean climate variability using a coupled regional climate system model. Clim. Dyn. **44**, 1127–1155 (2015)
25. Conradie, E.H., Van Zyl, P.G., Pienaar, J.J., Beukes, J.P., Galy-Lacaux, C., Venter, A.D., Mkhatshwa, G.V.: The chemical composition and fluxes of atmospheric wet deposition at four sites in South Africa. Atm. Environ **146**, 113–131 (2016)